The interplay between the lattice and magnetism in $La(Fe_{11.4}Al_{1.6})C_{0.02}$ studied by powder neutron diffraction*

Wang Zhi-Cui(王志翠)[a)b)], He Lun-Hua(何伦华)[b)], Wang Hai(王 海)[a)], Liu Rong-Deng(刘荣灯)[c)], and Wang Fang-Wei(王芳卫)[b)†]

[a)] *Magneto-Optic Thin Film Laboratory, Department of Physics, Capital Normal University, Beijing* 100037, *China*

[b)] *ECTSI/CSNS, Beijing National Laboratory for Condensed Matter Physics, Institute of Physics, Chinese Academy of Sciences, Beijing* 100190, *China*

[c)] *China Institute of Atomic Energy, Beijing* 102413, *China*

(Received 4 January 2012; revised manuscript received 10 January 2012)

The crystallographic structure and magnetic properties of $La(Fe_{11.4}Al_{1.6})C_{0.02}$ are studied by magnetic measurement and powder neutron diffraction with temperature and applied magnetic field. Rietveld refinement shows that $La(Fe_{11.4}Al_{1.6})C_{0.02}$ crystallizes into the cubic $NaZn_{13}$-type with two different Fe sites: Fe^{I} (8b) and Fe^{II} (96i), and that Al atoms preferentially occupy the Fe^{II} site. A ferromagnetic state can be induced at a medial temperature of 39 K–139 K by an external magnetic field of 0.7 T, and a large lattice is correspondingly found at 100 K and 0.7 T. In all other conditions, $La(Fe_{11.4}Al_{1.6})C_{0.02}$ has no net magnetization in the paramagnetic ($T > T_N = 182$ K) or antiferromagnetic states, and thus keeps its small lattice. Analysis of the Fe–Fe bond length indicates that the ferromagnetic state prefers longer Fe–Fe distances.

Keywords: neutron diffraction, crystallographic structure, magnetic phase transition

PACS: 61.05.F–, 83.10.Tv **DOI:** 10.1088/1674-1056/21/4/046101

1. Introduction

Magnetic refrigeration at room temperature is of particular interest because of energy saving and environmental protection. Among the materials showing a large magnetocaloric effect (MCE), Fe-based intermetallic compounds with a cubic $NaZn_{13}$-type structure (space group: $Fm\bar{3}c$) are attracting renewed interest due to a large MCE and low cost.[1−6] In the hypothetical $LaFe_{13}$, 13 Fe atoms are located at two symmetric sites, Fe^{I} at 8b(0, 0, 0) and Fe^{II} at 96i(0, y, z), in a ratio of 1:12. One central Fe^{I} atom and its nearest neighbours of 12 Fe^{II} atoms form a cluster. La atoms at 8a(1/4, 1/4, 1/4) are surrounded by 24 Fe^{II} atoms. The pseudo-binary intermetallic compounds, $La(Fe,Al/Si)_{13}$, crystallize into the $NaZn_{13}$-type structure by substituting Al or Si for part of the Fe. $LaFe_{13-x}Al_x$ compounds exhibit a unique magnetic phase diagram at different x values.[7] For the low Al-doped compounds ($1 < x < 2$), an antiferromagnetic (AFM) ground state was proposed by neutron diffraction,[8] where the AFM coupling is established between the (100) planes, while the ferromagnetic (FM) coupling is kept for all the Fe_{13} clusters in the (100) planes. This AFM coupling seems to result from the short Fe–Fe distance between the Fe_{13} clusters.[9]

For $La(Fe_{11.4}Al_{1.6})C_{0.02}$, a transition from the AFM ground state to the FM state, induced by an applied magnetic field, was recorded by magnetization measurements.[10] The magnetic-field-induced first-order transition, usually accompanied with a structural phase transition, was initially predicted by Wohlfarth and Rhodes on the basis of the collective electron model in the1960s, 50 years ago.[11] For example, an irreversible magnetic-field-induced AFM–FM transition in $R_5(Ge,Si)_4$, another system with giant room-temperature MCE, is accompanied by a

*Project supported by the National Basic Research Program of China (973 Program) (Grant No. 2010CB833102) and the National Natural Science Foundation of China (Grant No. 10974244).

†Corresponding author. E-mail: fwwang@aphy.iphy.ac.cn

© 2012 Chinese Physical Society and IOP Publishing Ltd

martensite-type structural transition.[12−14] Similarly, in La(Fe,Al/Si)$_{13}$ system, a first-order lattice expansion is also companied by FM ordering, although the crystallographic symmetry holds. In this paper, neutron diffraction and the Rietveld technique were employed to extensively check this interplay between lattice and magnetism in La(Fe$_{11.4}$Al$_{1.6}$)C$_{0.02}$.

2. Experiment

Sample La(Fe$_{11.4}$Al$_{1.6}$)C$_{0.02}$ was first prepared by arc melting in an argon atmosphere of high purity using the raw materials of La, Fe, Al, and an Fe–C alloy of at least 99.9% purity. After repeated arc melting, the alloyed button was annealed at 1223 K in a vacuum quartz tube for two weeks. Room-temperature X-ray diffraction was employed to check the phase composition and basic crystallographic structure. The annealed compound crystallizes into the NaZn$_{13}$-type structure with some amount of α-Fe as a secondary phase. The magnetic measurements were performed on a commercial superconducting quantum interference device magnetometer (SQUID, quantum design MPMS-7). Neutron diffraction was carried out on the diffractometer WAND, installed at the reactor HIFR of Oak Ridge National Laboratory, USA. The incident beam of the wavelength $\lambda = 0.1478$ nm was monochromatized by Ge (113). Three patterns were recorded at 220, 100, and 5 K in a low field of 0.01 T, and then four patterns at 220, 160, 100, and 5 K in a field of 0.7 T. Data were collected over the range $2\theta = 10°$–$138°$ with a step increment of 0.2°, and analysed by the Rietveld technique via the FULLPROF program.[14]

3. Results and discussion

Figure 1 shows the temperature dependences of the magnetization (i.e. the M–T curve) of La(Fe$_{11.4}$Al$_{1.6}$)C$_{0.02}$ under the fields of 0.01 T and 0.7 T. With increasing temperature, one can find three magnetic phase transitions in the 0.7 T field at $T_{c1} = 39$ K, $T_{c2} = 139$ K, and $T_{c3} = 182$ K, while only two phase transitions at 100 K and 182 K are observed in 0.01 T, as shown in the inset of Fig. 1. These results are consistent with the previous work.[10] Considering the AFM in La(Fe$_{0.91}$Al$_{0.09}$)$_{13}$ detected by neutron diffraction,[8] we speculate that the ground state of La(Fe$_{11.4}$Al$_{1.6}$)C$_{0.02}$ is an unstable AFM state, and this instability can be broken by temperature and external field. In low field, La(Fe$_{11.4}$Al$_{1.6}$)C$_{0.02}$ changes from the unstable AFM ground state low temperatures to a relatively robust AFM state. Under 0.7 T, the unstable AFM ground state jumps to a ferromagnetic state at T_{c1}, then drops to the robust AFM state at T_{c2}. The paramagnetism can be reached with $T > T_{c3}$ (=182 K, i.e. Neel temperature), and the temperature does not shift under the applied field of 0.7 T.

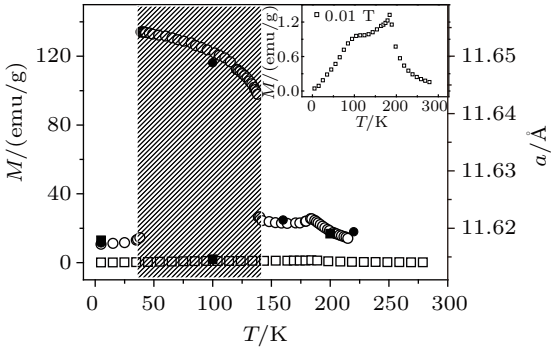


Fig. 1. Magnetization M and lattice parameter a as a function of temperature under different applied magnetic fields (□: M at 0.01 T, ◯: M at 0.7 T; ■: a at 0.01 T, ●: a at 0.7 T). Inset: the M–T data in 0.01 T with a small scale.

The Rietveld technique was employed to analyse the neutron diffraction data. The location of carbon atoms cannot be refined due to a quite low concentration, thus the fixed occupancy on the 24d site is adopted as N atoms in La(Fe$_x$Al$_{1-x}$)$_{13}$.[15] The phase composition and Al occupancy are extracted from the pattern of the paramagnetic state (220 K, 0.01 T) first, and verified by analysing all others patterns. The refinement shows that the annealed La(Fe$_{11.4}$Al$_{1.6}$)C$_{0.02}$ crystallizes in an NaZn$_{13}$-type cubic structure with α-Fe as a secondary phase. Al atoms prefer only the Fe$^{\rm II}$(96i) site with the occupancy of 14(±2)%, thus $x = 1.7(\pm 0.2)$, in coincidence with the starting stoichiometric ratio. This preferential occupation is consistent with previous studies in La(Fe$_{1-x}$Al$_x$)$_{13}$,[16−18] but in conflict with the random distribution of Si atoms at both Fe$^{\rm I}$ and Fe$^{\rm II}$ sites in the Si-doped La(Fe,Si)$_{13}$ compounds.[19,20] Generally, the positive alloying heat between La and Fe is considered to be the reason why no La–Fe binary compound exists.[21] Since the La atom is surrounded by the Fe$^{\rm II}$ atoms, this preferential occupancy of Al atoms can lower the formation heat effectively, which helps the formation of the NaZn$_{13}$ phase.

We also attempt to determine the spin configuration of $La(Fe_{11.4}Al_{1.6})C_{0.02}$ from the low-temperature patterns. Regrettably, it cannot be figured out from our diffraction data due to two limits of the WAND. For the AFM state, the low angles ($2\theta < 10°$) to record the AFM superlattice peak are not obtained. For the FM state, the ferromagnetic reflections, superposed on the lattice Bragg peaks, contribute only less than 5% intensity in total for the $NaZn_{13}$-type structure, but the WAND's medium resolution fades them out. Consequently, only the crystallographic structure has been refined for all data series. The refined patterns are statistically agreed with the observed data as examples plotted in Fig. 2. The refined crystallographic parameters are summarized in Table 1.

Table 1. The structural data of $La(Fe_{11.4}Al_{1.6})C_{0.02}$ from the Rietveld analysis at several temperatures under 0.01 T and 0.7 T.

	0.01 T			0.7 T			
	5 K	100 K	220 K	5 K	100 K	160 K	220 K
a/Å	11.618(2)	11.615(2)	11.619(8)	11.617 (2)	11.649(2)	11.621 (2)	11.619 (2)
Fe^{II} $(0, y, z)$							
y	0.1787(2)	0.1785(2)	0.1783(2)	0.1787(2)	0.1788(2)	0.1783(2)	0.1782(2)
z	0.1157(2)	0.1157(2)	0.1158(2)	0.1156(2)	0.1154(2)	0.1157(2)	0.1157(2)
Bond lengths/Å							
La–Fe^{II}	3.399(2)	3.399(2)	3.400(2)	3.400(2)	3.410(2)	3.401(2)	3.401(2)
Fe^{I}–Fe^{II}	2.473(2)	2.471(2)	2.470(2)	2.473(2)	2.479(2)	2.470(2)	2.469(2)
Fe^{II}–Fe^{II}: B1(1)	2.688(3)	2.688(3)	2.691(3)	2.688(3)	2.689(3)	2.689(3)	2.689(3)
B2(4)	2.579(3)	2.576(2)	2.575(2)	2.579(2)	2.587(2)	2.575(2)	2.573(2)
B3(2)	2.522(3)	2.524(3)	2.529(3)	2.521(3)	2.523(3)	2.528(3)	2.530(3)
B4(2)	2.498(3)	2.499(3)	2.500(3)	2.498(3)	2.509(3)	2.502(3)	2.502(3)
R_{wp}/%	15.4	15.8	15.8	15.6	15.7	14.5	14.2

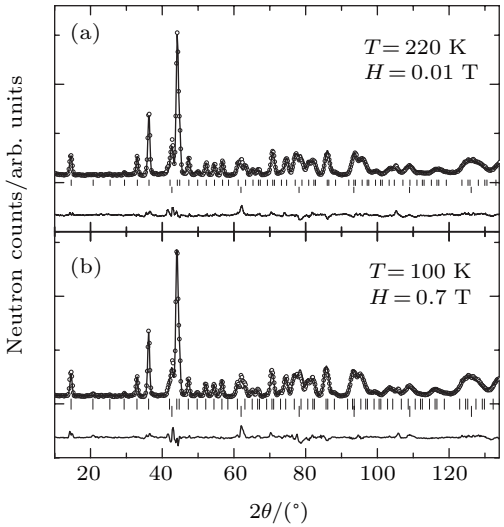


Fig. 2. Observed (circle) and calculated (line) neutron diffraction patterns and their difference of $La(Fe_{11.4}Al_{1.6})C_{0.02}$ at (a) 0.01 T, 220 K, and (b) 0.7 T, 100 K.

Although the magnetic structure cannot be determined from the diffraction data, the lattice change seems to give us a track about the transition of magnetic configuration since a strong interplay between the lattice and magnetism has been concluded in the related system.[9,19,20] The temperature-dependent lattice parameter a of $La(Fe_{11.4}Al_{1.6})C_{0.02}$ is also plotted in Fig. 1 with the M–T curves. Apparently, the lattice parameter is strongly coupled with the macroscopic net magnetization. The small lattice is accompanied by no net magnetization state, even paramagnetism at high temperatures or AFM in low field, whereas the large lattice is triggered by a net magnetization of the FM state at 100 K and 0.7 T. The FM lattice parameter increases by $\sim 0.26\%$ from the PM or AFM one, and the unit-cell volume expands $\Delta V/V = 0.78\%$ if the first-order approximation $\Delta V/V = 3\Delta a/a$ is considered. In the Si-substituted $La(Fe,Si)_{13}$ system, the linear lattice-volume dependence[22] and no H/D isotope effect[23] suggest that only the magneto volume effect is responsible for this strong interplay between lattice and magnetism. However, the difference between the Al-doped system and the Si-doped one is worth noting. For $La(Fe_{11.4}Al_{1.6})C_{0.02}$ and $LaFe_{11.4}Si_{1.6}$, two compounds with the same Al/Si doping concentration, the lattice parameter $a = 11.61788$ Å (1 Å=0.1 nm) at 5 K for $La(Fe_{11.4}Al_{1.6})C_{0.02}$ is about 1% larger than $a = 11.5328$ Å at 2 K for $LaFe_{11.4}Si_{1.6}$. But

$La(Fe_{11.4}Al_{1.6})C_{0.02}$ is the AFM ground state and $LaFe_{11.4}Si_{1.6}$ the FM one. This seems to imply that electronic transfer between Fe and Al/Si atoms, and thus an energy band change, also plays an important role in the magnetic properties in the $La(Fe,Al/Si)_{13}$ family.

The bond lengths, calculated from the crystallographic data in Table 1, are plotted in Fig. 3 as a function of temperature, where the Fe–Fe bond lengths are classified into three types: Fe^{I}–Fe^{II}, the intra-cluster Fe^{II}–Fe^{II} (B1, B2, and B1>B2), and inter-cluster Fe^{II}–Fe^{II} (B3, B4, and B3>B4). FM ordering (100 K, 0.7 T) gives rise to an elongation of the bond lengths of La–Fe^{I} (0.29%) and, relatively, the Fe–Fe bond lengths in each type: 0.32% for Fe^{I}–Fe^{II}, 0.43% for B2, and 0.36% for B4, respectively, but has no effect on B1 and B3. However, as for the temperature dependence of the lattice parameter, the AFM ordering has no obvious effect on bond length. It can be concluded that the ferromagnetism of $La(Fe_{11.4}Al_{1.6})C_{0.02}$ also prefers the longer Fe–Fe bond lengths as in the $La(Fe,Si)_{13}$ system.[19] It is well known that small Fe–Fe distances in densely packed Fe-based alloys usually result in a pronounced tendency towards antiferromagnetic exchange interaction.[24] Small bond lengths of Fe^{I}–Fe^{II}, and the inter-cluster Fe^{II}–Fe^{II}, might be the reason why $La(Fe_{11.4}Al_{1.6})C_{0.02}$ has an AFM ground state.

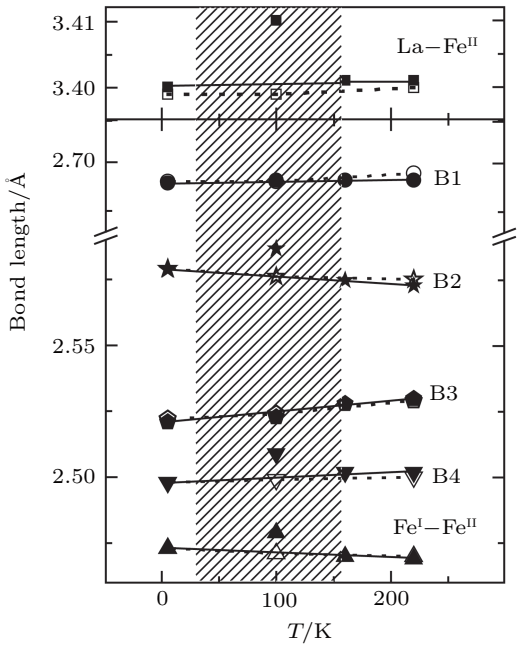


Fig. 3. The bond lengths of $La(Fe_{11.4}Al_{1.6})C_{0.02}$ as a function of temperature in a field (solid symbol: 0.7 T, open symbol: 0.01 T). The shadow shows the temperature range where the ferromagnetism is induced by 0.7 T.

4. Conclusions

The interplay between the lattice and magnetism in $La(Fe_{11.4}Al_{1.6})C_{0.02}$ has been investigated by magnetic measurement and powder neutron diffraction. Rietveld refinement shows that $La(Fe_{11.4}Al_{1.6})C_{0.02}$ crystallizes into the cubic $NaZn_{13}$-type, and Al atoms preferentially occupy the Fe^{II} site. The FM state is induced by an external magnetic field of 0.7 T in the medial temperature of 39 K–139 K, and the lattice expands correspondently. For the paramagnetic ($T > T_N = 182$ K) or antiferromagnetic states, it has no net magnetization, and thus keeps its small lattice. Analysis of the Fe–Fe bond lengths also indicates that small bond lengths of Fe^{I}–Fe^{II} and the inter-cluster Fe^{II}–Fe^{II} might be the reason why $La(Fe_{11.4}Al_{1.6})C_{0.02}$ has an AFM ground state. But electronic transfer between Fe and Al atoms also plays an important role.

Acknowledgments

The authors wish to thank Dr. Hong-Wei Zhang of IOP, China, for preparing the sample, and Dr. J A Fernandez-Baca of Oak Ridge National Laboratory, USA, for collecting the neutron data.

References

[1] Gschneidner Jr K A, Pecharsky V K and Tsokol A O 2005 *Rep. Prog. Phys.* **68** 1479
[2] Brück Ekkes 2005 *J. Phys.* D: *Appl. Phys.* **38** R381
[3] Pecharsky V K and Gschneidner Jr K A 1997 *Phys. Rev. Lett.* **78** 4494
[4] Pecharsky V K and Gschneidner Jr K A 1997 *Appl. Phys. Lett.* **70** 3299
[5] Tegus O, Brück E, Buschow K H J and de Boer F R 2002 *Nature* **415** 150
[6] Zhang X X, Wen G H, Wang F W, Wang W H, Yu C H and Wu G H 2000 *Appl. Phys. Lett.* **77** 3072
[7] Palstra T T M, Nieuwenhuys G J, Mydosh J A and Buschow K H J 1984 *J. Appl. Phys.* **55** 2367
[8] Helmholdt R B, Palstra T T M, Nieuwenhuys G J, Mydosh J A, van der Kraan A M and Buschow K H J 1986 *Phys. Rev.* B **34** 169
[9] Hu F X, Shen B G, Sun J R, Cheng Z H, Rao G H and Zhang X X 2001 *Appl. Phys. Lett.* **78** 3675
[10] Zhang H W, Chen J, Liu G J, Zhang L G, Sun J R and Shen B G 2006 *Phys. Rev.* B **74** 212408
[11] Wohlfarth E P and Rhodes P 1962 *Phil. Mag.* **7:83** 1817
[12] Tsutaoka Takanori, Tanaka Akira, Narumi Yasuo, Iwaki Masahiro and Kindo Koichi 2010 *Physica* B **405** 180
[13] Tang H, Pecharsky V K, Gschneidner Jr K A and Pecharsky A O 2004 *Phys. Rev.* B **69** 064410
[14] Mudryk Ya, Holm A P, Gschneidner Jr K A and Pecharsky V K 2005 *Phys. Rev.* B **72** 064442

[15] Moze O, Kockelmann W, Liu J P, de Boer F R and Buschow K H J 2000 *J. Appl. Phys.* **87** 9

[16] Dong Q Y, Chen J, Zhang H W, Sun J R and Shen B G 2008 *J. Phys.*: *Condens. Matter* **20** 275235

[17] Dong Q Y, Zhang H W, Sun J R and Shen B G 2008 *J. Phys.*: *Condens. Matter* **20** 135205

[18] Chen J, Zhang H W, Zhang L G, Dong Q Y and Wang R W 2006 *Chin. Phys.* **15** 845

[19] Wang F W, Wang G J, Hu F X, Kurbakov A, Shen B G and Cheng Z H 2003 *J. Phys.*: *Condens. Matter* **15** 5269

[20] Wang F W, Kurbakov A, Wang G J, Hu F X, Shen B G and Cheng Z H 2006 *Physica* B **385** 343

[21] Miedema A R, de Châtel P F and de Boer F R 1981 *Physica* B **100** 1

[22] Jia L, Sun J R, Wang F W, Zhao T Y, Zhang H W, Shen B G, Li D X, Nimori S, Ren Y and Zeng Q S 2008 *Appl. Phys. Lett.* **92** 101904

[23] Wang Z C, He L H, Cuevas F, Latroche M, Shen J and Wang F W 2011 *Chin. Phys.* B **20** 067502

[24] Coey J M D (ed.) 1996 *Rare-earth Iron Permanent Magnets* (Oxford: Clarendon) p. 512